Adaptive coded aperture imaging: progress and potential future applications

Stephen R. Gottesman*[a], Abraham Isser[a], George W. Gigioli, Jr.[a]

[a]Northrop Grumman Electronic Systems, 1745A. W. Nursery Rd., MS-1105, Linthicum, MD, USA 21090-2906

ABSTRACT

Interest in Adaptive Coded Aperture Imaging (ACAI) continues to grow as the optical and systems engineering community becomes increasingly aware of ACAI's potential benefits in the design and performance of both imaging and non-imaging systems , such as good angular resolution (IFOV), wide distortion-free field of view (FOV), excellent image quality, and light weight construct. In this presentation we first review the accomplishments made over the past five years, then expand on previously published work to show how replacement of conventional imaging optics with coded apertures can lead to a reduction in system size and weight. We also present a trade space analysis of key design parameters of coded apertures and review potential applications as replacement for traditional imaging optics. Results will be presented, based on last year's work of our investigation into the trade space of IFOV, resolution, effective focal length, and wavelength of incident radiation for coded aperture architectures. Finally we discuss the potential application of coded apertures for replacing objective lenses of night vision goggles (NVGs).

Keywords: Adaptive coded aperture imaging (ACAI), decoding algorithms, night vision goggles (NVGs), angular resolution, coded aperture imaging, image reconstruction, system point spread function (SPSF), MURAs

1. INTRODUCTION

Adaptive Coded Aperture Imaging (ACAI) has evolved over several years in different but complementary directions in terms of the hardware deployed and signal processing algorithms used to process the recorded data into a recognizable image. Traditional non-diffractive/non-adaptive coded aperture imaging was developed for imaging gamma-rays and x-rays where the ratio of wavelength to instrument feature size is sufficiently small that diffraction effects can be completely ignored. See for example the development of the URA [1]. In this regime an aperture consisting of open and opaque areas, or cells, modulates the incident flux instead of traditional refracting or reflecting optics, thus eliminating weight and complexity albeit at the expense of having to digitally process the focal plane data to transform it into a recognizable image. Early systems built in this configuration exhibited desirable imaging characteristics such as wide field-of-view (FOV) and good angular resolution, so it was only a matter of time before researchers considered applying the same techniques to the visible (VIS) and mid-wave IR (MWIR) portion of the electromagnetic spectrum. Some researchers were initially discouraged by the consideration that diffraction effects would now became appreciable due to the larger wavelength-to-aperture cell size ratio, especially for MWIR applications, thus rendering the technique ineffective, and little progress was made until relatively recently, particularly in the last five years, when it was realized that many of the undesirable effects related to diffraction could be mitigated by hardware design and signal processing. Systems have now been built and tested that operate at VIS and MWIR wavelengths. Some of the configurations are hybrids in the sense that they use refractive optics in addition to a coded aperture , and are 'adaptive' by changing the aperture pattern as part of the data acquisition process [2, 3]. The term 'Adaptive Coded Aperture Imaging' generally refers to configurations where diffraction is important and one or more of the above techniques are applied.

We report on our investigation into the application of ACAI technology to traditional imaging devices such as night vision goggles (NVGs). By investigating a 'strawman' point design we will gain insight into the effects of key engineering parameters such as aperture cell size, angular resolution, distance between aperture and focal plane, bandpass, sensitivity, and dispersion. ACAI could help reduce NVG weight by substituting a coded aperture for the device's objective lens. NVGs have been known to cause muscle strain on long deployments due to weight, a fact that calls for lighter devices.

*stephen.gottesman@ngc.com; phone 1 410 765-7442; fax 1 410 981-2819; www.northropgrumman.com

This paper is organized as follows. We first give a brief review of the non-diffractive case. We then review imaging in the diffractive regime and examine diffraction patterns simulated by Zemax [8] for Modified Uniformly Redundant Arrays, (MURAs). This knowledge is then applied to a NVG point design which we evaluate in terms of IFOV and system point spread function. We conclude by summarizing results and identifying areas requiring further research before a practical system can be confidently designed.

1.1 Geometric mode imaging

Figure 1 shows the aperture pattern of an NxN MURA with N=13 elements comprising the basic pattern (central square) and the larger physical aperture formed by replicating the basic pattern around itself as described in reference [4]. Not shown in the figure is the image plane (detection plane) located behind the aperture at distance (z). With the ratio (λ/b) sufficiently small that diffraction can be ignored, a point source located at infinity on the principal axis will project onto the image plane a replica of the aperture pattern, but by design only the central 13x13 portion is sampled by the detectors. The key feature in this implementation is that a complete cycle of the 'basic' 13x13 pattern is always projected and sampled on the image plane. Sources off axis will also project the aperture pattern onto the image plane but will be shifted in proportion to their angular displacement. An important feature of MURA apertures is that the set of shifted patterns are all orthogonal to each other under correlation. The recorded data will look nothing like an image, being essentially a sum of shifted aperture patterns, but the image is easily reconstructed by a cyclic correlation technique described in references [4, 5, and 6]. The advantage of using a MURA design as compared to random masks or other patterns has been discussed in the literature [6].
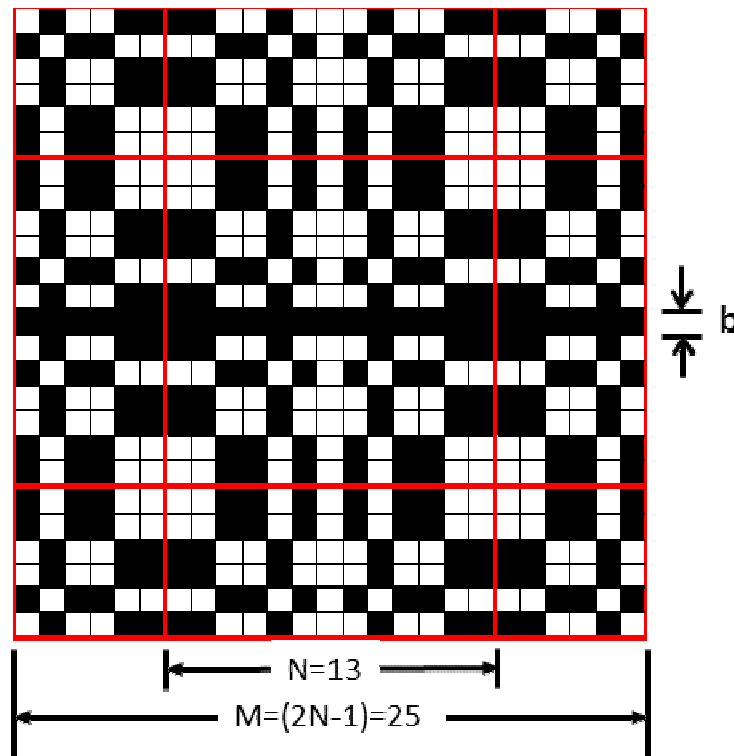

Figure 1. Conventional NxN MURA coded aperture with N=13. The 'basic' pattern is the central square which is 'mosaiced' around its periphery as explained in ref. [4].

The angular resolution of such a device determines how effectively two point sources can be distinguished from each other and can be calculated using equation (8) from reference [6]. In that article we showed the Instantaneous Field of View (IFOV) to be *b/z* and angular resolution, defined as the minimum resolving angle between two point sources, to be

$$\theta_{geom} = b/2z \quad . \tag{1}$$

We selected for this study a coded aperture system with $b = 71$ um and $z = 50$ mm. With these values inserted into equation (1) we have then

$$\theta_{geom} = 710 \ \mu rad. \tag{2}$$

Note that in this approximation there is no dependence on wavelength; angle resolution is determined entirely by the system's geometry.

1.2 Diffractive mode imaging

When λ/b is no longer negligible, diffraction will dominate and we must then consider its effect at the focal plane. For a single aperture hole of dimension (b) the well-known Rayleigh criterion is

$$\Theta_{diff} = 1.22\lambda/b = 13.7 \ mrad \tag{3}$$

which is significantly larger than the geometric resolution given by equation (2). Since most tactical systems require one mrad or less angular resolution, diffraction appears to render coded apertures useless in this regime. However in reference [6] we argue this conclusion to be false and claim the corrected equation to be

$$\Theta_{diff} = 1.22\lambda/Mb = 1.22\lambda/25b = 550 \ \mu rad. \tag{4}$$
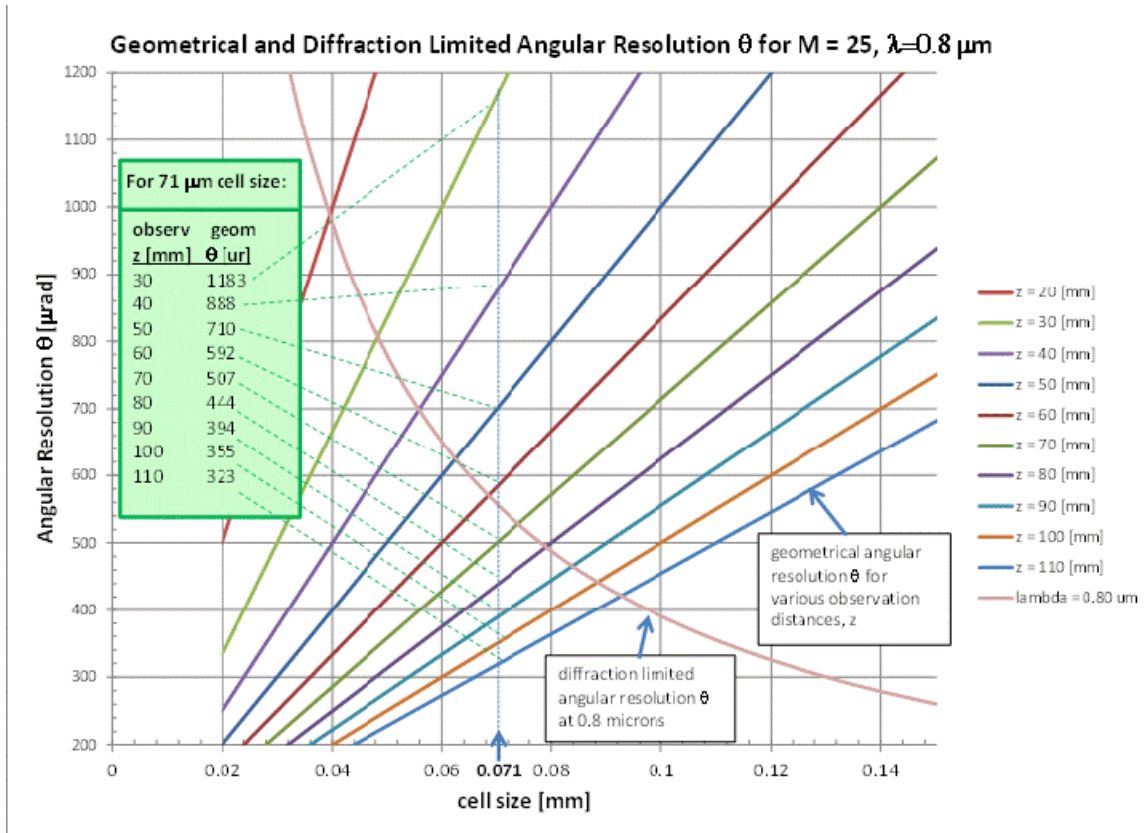

Figure 2. Angular resolution versus aperture cell size for different distances (z) separating aperture and focal plane for 800 nm incident wavelength.

In effect the entire aperture behaves as a diffraction grating so that the principal diffraction peaks will have a width of approximately (*1/M*) of what would be obtained with a single hole, where (*M*) is the number of aperture elements in one dimension, see Figure 1.

The significance of this is enormous since feature sizes on the focal plane will now be constrained and therefore decoding techniques developed for the geometric case may be valid in some modified sense even though the system is operating in the diffraction mode.

Figure 2 shows angular resolution as a function of aperture cell size and focal plane distance for 800 nm incident light typical of night vision goggles. The straight lines represent results for different aperture-to-focal plane distance. They show a simple linear relationship between cell size (b) and angular resolution (θ). These values were generated using equation (1). Superimposed on this plot is the diffraction limited curve. When designing a system one must pay attention to stay above this curve.

The designer must also consider the effects of optical dispersion which further limits angular resolution to the following value:

$$\theta res = \sqrt{(\Delta\lambda/2z)} \tag{5}$$

This relationship was derived in [6]. $\Delta\lambda$ refers to the system's bandpass which we have set at $\Delta\lambda = 100$ nm, and (z) is still the distance separating the aperture from the focal plane which we take to be z = 50 mm. Substituting these values into the formula yields

$$\theta_{res} = 1 \, mrad. \tag{6}$$

The system's operating resolution will be limited by the largest of the three (Eq.2, Eq.4, and Eq.6).

The key design parameter values, $b = 71$ μm, $z = 50$ mm, $\lambda = 800$ nm, and $\Delta\lambda = 100$ nm, were chosen to yield images comparable to those obtained with night vision goggles as shown in the next section.

2. CODED APERTURE IMPLEMENTATION TO NIGHT VISION GOGGLES (NVGS)

2.1 Discussion of current Gen 4 NVG hardware

We now devote our attention to the application of coded apertures to night vision goggles. The idea is to replace the front optic with a coded aperture to reduce device physical weight and user muscle strain. Before proceeding we review the basic operating principles and performance of NVGs.

NVGs consist of several main components: an objective lens, an eyepiece, a power supply and an image intensifier tube with a photocathode. An illustrated cross section of a NVG and a 4th Gen Night Vision Goggle are shown in figure 3. See reference [7] for details.

Night vision devices gather existing ambient light (starlight, moonlight or near infra-red light) through the front lens. This light, consisting of photons in the visible and Near Infra Red band (VNIR) part of the spectrum, is focused onto a photocathode that converts the photons to electrons. The electrons are then amplified to a much greater number after passing through a Multi Channel Plate (MCP) and then accelerate towards a phosphor screen that changes the amplified electrons back into visible light observed by the user through an eyepiece. The resultant image will be a clear green-hued amplified re-creation of the low light outside scene. NVGs can be either 1st, 2nd, 3rd or 4th generation units. The generation refers to the type of image intensifier used for that particular device.

Fourth generation (4th GEN) devices use gated filmless inverting image intensifier tubes to improve night operational effectiveness. The filmless MCP provides a higher signal-to noise ratio than standard 3rd Gen. NVGs, resulting in better image quality under low-light conditions. A gated power supply further improves image resolution under high light conditions and reduces the halo effect caused by interference from bright light sources enabling effective night vision operation in dynamic lighting conditions such as urban areas.

For the purpose of analysis, we considered a state of the art high performance 4th Gen. NVG with the following features:

- Photo Cathode type: Filmless GaAs
- Resolution of up to 72 line pairs/mm (approximately 1/3 to 2/3 mrad IFOV assuming a 2.5 cm focal distance for the human eye.)
- Signal-to-Noise Ratio up to 30
- NVG Length: 12 cm
- NVG Weight: 4.25 lbs

A dual night vision goggle system, shown in Figure 3, utilizes two Gen. 4 high performance image intensifier tubes to enable high resolution low light level imagery as well as improved depth perception needed for night driving and navigation and aircraft pilotage. While high quality NVG imagery is critical for night missions, NVG's weight is a critical factor in overall mission effectiveness.

Weight reduction of NVGs is a key factor in reducing operator fatigue and in enhancing operator effectiveness. The weight of a heavy 4.25 lbs NVG could be potentially reduced down to less than 3 lbs by replacing the heavy objective lens with a light weight film based coded aperture and replacing the phosphor screen with a thin LCD display. A typical 1X objective lens could weigh as much as ~30% of the overall NVG weight, and higher magnification objective lenses with 3X or 5X magnification factors could exceed 50% of the NVG overall weight.
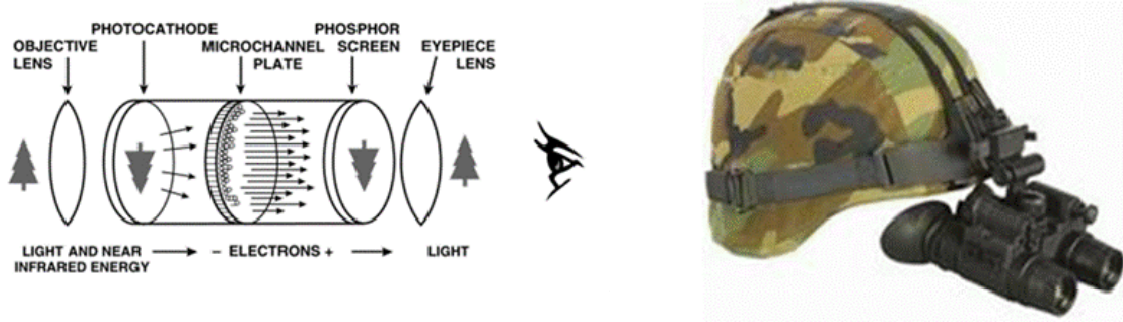

Figure 3. NVG components (left) from [7] and a helmet equipped with dual 4th Gen NVGs.

2.2 Conceptual design

The current state-of-the-art 4th generation NVGs multiply the light gathering power of the eye or video receptor up to >50,000 times. A typical GEN 4 NVG is characterized by a Gallium Arsenide (GaAs) photocathode. The photon sensitivity of the GaAs photocathode extends into the near-infrared region, where night sky radiance and contrast ratios reach peak values.

The GaAs photocathode reaches peak sensitivity between 800-950 nanometers and is well matched with the night sky peak spectral glow. This spectral response shift to the red region results in improved Signal-to-Noise Ratio and in significant improvement in visual acuity and detection distances when compared with Gen 1 and Gen 2 NVGs.

In order to reduce weight we propose replacing the objective lens with a coded aperture, and the phosphor screen with a LCD display that is connected to an image processor. The Image processor will decode the projected coded aperture illumination and convert it to a reconstructed image of the scene. The processing power of the image processor must be sufficient to reconstruct the images in real time.

The coded aperture design chosen for replacing the objective lens of a Gen 4 NVG was analyzed for the following design parameters:

- Central Wavelength of operation (λ): 800nm
- Wavelength bandpass ($\Delta\lambda$): 100nm (750nm-850nm)
- Coded aperture cell size (b): 71 microns (um)
- Coded aperture focal distance (z) 50 mm

As shown in Section 1.2, Eq.6, the coded aperture parameters chosen for this configuration produce an angular resolution of approximately 1 mrad. The limiting factor appears to be optical dispersion caused by the 100 nm bandpass. A narrower bandpass would improve resolution but at the expense of light collection and hence decrease sensitivity, so a 100 nm bandpass was chosen as the nominal value for this configuration.

3. EVALUATION OF PERFORMANCE

The coded aperture shown in Figure 1 was selected for this study based on several considerations. The number of aperture cells in the simulation, being only 25x25=625 in number, should be adequate without being unwieldy. It is also symmetric and balanced (50% open, 50% closed), an advantage when operating in 'dual frame' mode where data is acquired sequentially by alternating between one pattern and its complement to reduce image processing noise. Furthermore the underlying mathematical structure of the MURA carries over to larger arrays that will be needed for real-world applications such as NVGs, so lessons learned with the smaller arrays will be useful for studying the larger. Given the fact that the number of resolution elements in the reconstructed image will equal the number of elements in the basic pattern (13x13), the reconstructed image will only have 13 useful resolution elements in each dimension. It can however be scaled up to the roughly 1000 needed for a useful system with a 57 degree field of view (FOV) at 1 mrad IFOV. To verify that results obtained with the 13x13 aperture do scale to larger ones, we also modeled a 37x37 MURA.

In all cases aperture cells were oversampled by a factor of 5 in each dimension to ensure fidelity. The collection of focal plane sampling points can be thought of as a detector array consisting of 125x125 detectors with a pitch of

$$pitch = b/5 = 70.17/5 \, \mu m = 14.14 \, \mu m. \tag{7}$$

3.1 Image plane diffraction pattern generation

The image plane patterns presented in this paper represent monochromatic point spread functions (PSFs) of the aperture masks, including the effects of diffraction. These patterns were computed using the Physical Optics Propagation (POP) tool in the Zemax optical system design and analysis software package [8]. Because there are no refractive or reflective elements, the Zemax model consists of only three surfaces: the object plane; the mask; and the observation (or image) plane. The object is modeled as a point source at infinity to simulate a plane wave at the aperture. The mask is placed at the system aperture and the image plane is 50 millimeters beyond the mask.

The detailed structure of the mask is represented in the model as User Defined Aperture (UDA) associated with the aperture surface. The UDA file was generated with a simple Matlab program that converts a table of "1's" and "0's" into an aperture function with the proper file format recognized by Zemax. The mask cell dimensions are selected as inputs to the Matlab program. Essentially, the UDA file defines a set of rectangular aperture elements with the correct size and location of each to represent one transmitting unit cell of the MURA pattern. Together this set of rectangular apertures comprises the overall pattern. The entrance pupil diameter of the system is then specified to be large enough to overfill the aperture pattern. The size and geometry of the aperture mask is easily verified in Zemax by plotting the footprint diagram at the aperture plane surface.

In the POP tool of Zemax the X- and Y-Sampling were set to 4096. The X- and Y-Widths were set to a value that resulted in X and Y point spacing in the computed distribution that were five times smaller than the unit cell of the MURA pattern. Thus the pattern was guaranteed to be adequately sampled. Note that the X- and Y-Widths specified in this manner were significantly smaller than what is automatically computed by the POP program (i.e., smaller than the values computed when the Auto button is depressed in the Beam Definition tab of the POP Settings dialog box for a given aperture size). The Beam Type is specified to be a Top Hat, with the Waist X and Waist Y set equal to half of the system entrance pupil diameter.

Figure 4 shows the diffraction pattern (right) predicted by Zemax for plane wave illumination of the MURA (left) as observed at a focal plane placed 50 mm behind the aperture. The red lines demarcate a central region corresponding to the focal plane's sampled area and also to the 'basic' portion of the aperture. It is observed that four intensity peaks form at the corners of the FPA where the red lines intersect. The origin of this curios effect may be the aperture's resemblance to a zone plate, mosaicked into a 2x2 pattern, with each peak located on each zone plate center.
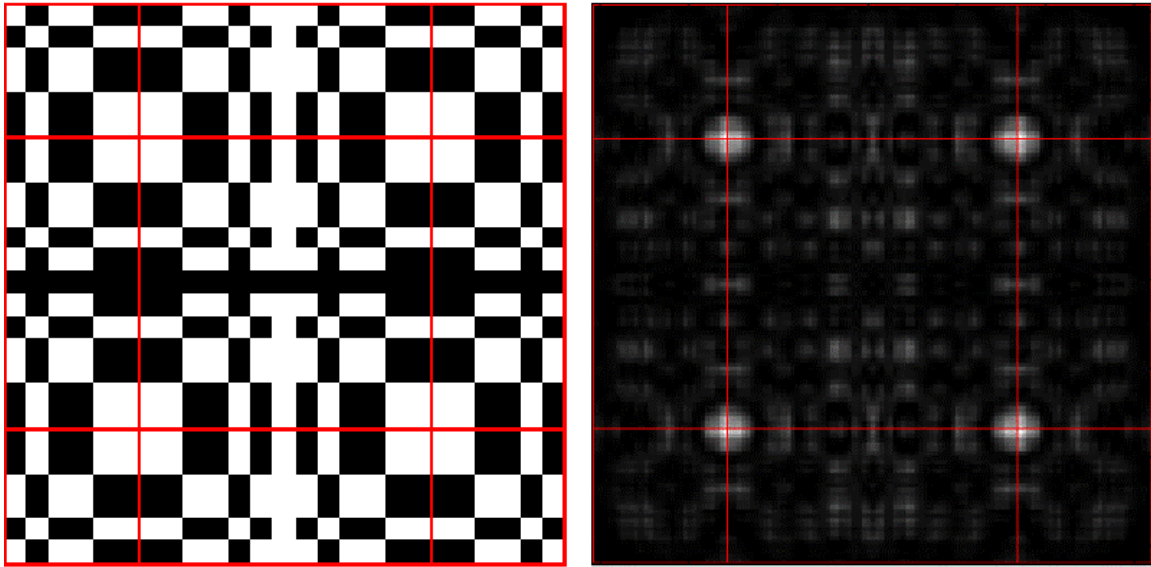
3.2 Image reconstrction

Figure 4. Diffraction pattern (right) detected on focal plane at z=50 mm for the 13x13 MURA aperture on left.

Image reconstruction may be carried out, at least to first approximation, by correlating the measured focal plane data with a kernel obtained from the central region of Figure 4. The kernel's auto-correlation function is essentially the system's point spread function (SPSF) where we are treating the system as including only an aperture in front of an array of ideal detectors. No consideration is given at this point to the MTF representing additional system components such as the MCP, LCD display, objective lens, and human eye. Figure 5 shows the SPSF, the system's response to a point source located at infinity.
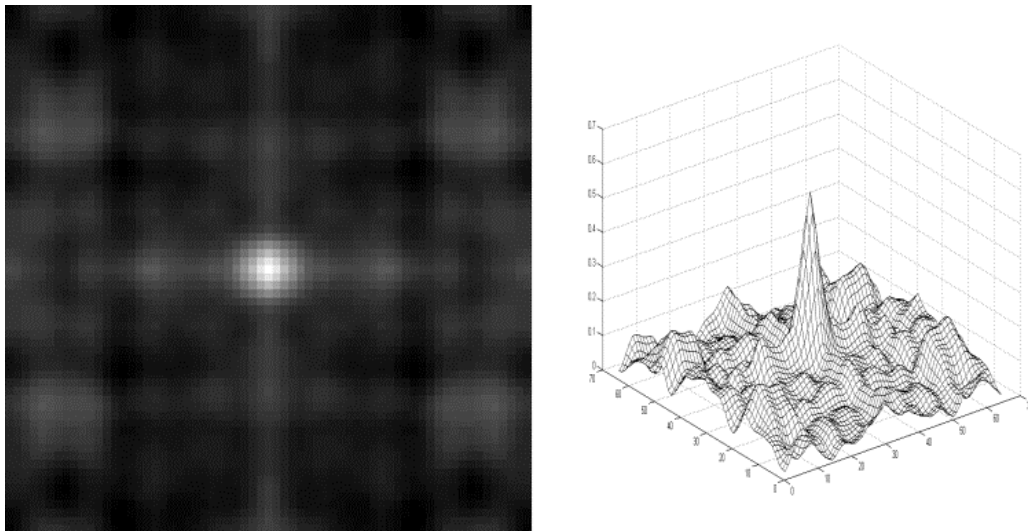

Figure 5. System Point Spread Function (SPSF) for the 13x13 MURA as intensity (left) and mesh (right) plots.

The SPSF is not perfect for it contains sidelobes that introduce artifacts and reduce SNR. Ideally we would like to eliminate the sidelobes completely, as is done with MURAs operating in the geometric regime, by 'inverting' the aperture function, but this has not yet been achieved with diffraction since the patterns it generates differ from the aperture's and are more difficult to invert. Exploitation of the pattern's symmetry may help in achieving this goal and is the subject of further research.

Nevertheless the SPSF is a peaked with a FWHM of approximately 5 detectors, which for a pitch of 14.1 um and a focal distance of 50 mm corresponds to approximately 1.4 mrad. Figure 6 shows the reconstructed image (left) of two point sources separated by 1.4 mrad (right).
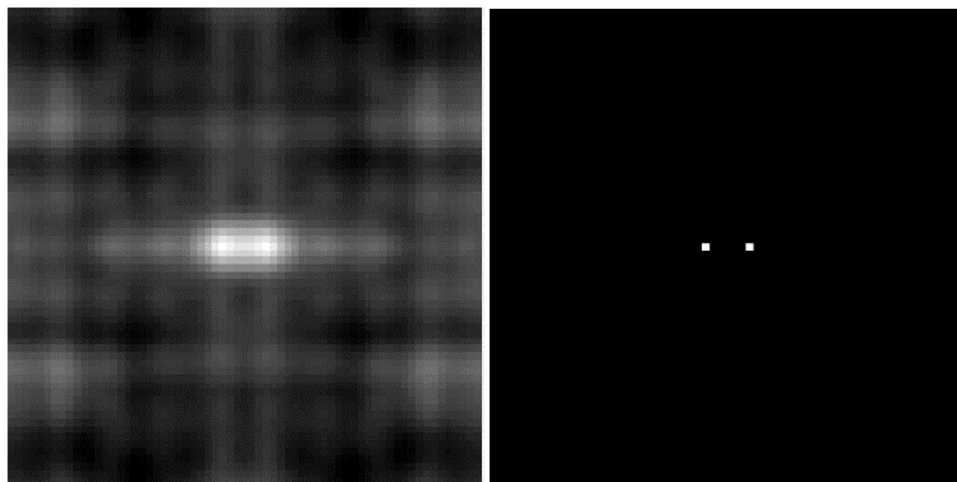

Figure 6. Reconstructed image (left) of two point sources separated 1.4 mrad (right) in angle space.

Figure 7 shows a 37x37 MURA aperture and its SPSF that should be compared to Figure 5. The FWHM of the peak is the same as for the 13x13 MURA and hence image quality will also be similar. The reader should note that the larger aperture increases the FOV but not the IFOV since all other system parameters remain unchanged. To reduce the IFOV either the observation distance (z) must be increased and/or the aperture cell size dimension (b) made smaller, while at the same time making sure that dispersion doesn't increase beyond tolerable limits due to the reduced (z). Likewise the diffraction curve given by equation 4 must also be monitored to make sure it doesn't increase beyond tolerable limits due to decreasing cell size (b), but for large M of order of 1000 should not be a problem.
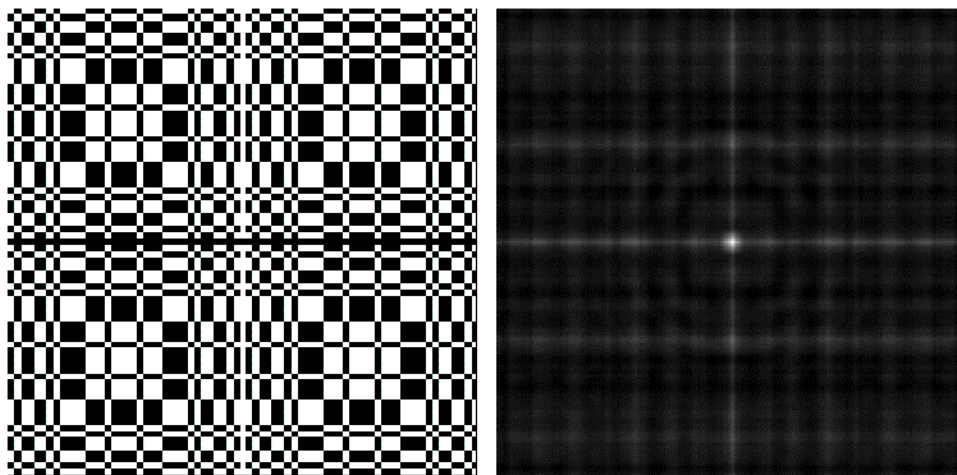

Figure 7. A 37x37 MURA aperture pattern (left), and its system point spread function (SPSF).

4. SUMMARY AND CONCLUSION

We have investigated the imaging qualities of two MURA coded apertures in terms of their system point spread functions (SPSFs) with the goal of ultimately replacing the objective lens in night vision goggles. The decoding

algorithm was to correlate the aperture diffraction kernel with the recorded scene. For this technique to be successful the diffraction pattern should replicate the central region. Close examination of Figure 4 shows this condition is not satisfied everywhere, particularly along the periphery, and this will degrade performance. By modifying the mosaicking process by which the aperture is constructed to include more repetitions of the basic pattern may be a way of solving this problem.

System parameters were chosen to yield approximately 1 mrad IFOV implying angular resolution of this amount or less. However our simulation suggests a value closer to 1.4 mrad for this design. The reconstructed images have artifacts as a consequence of the SPSF's sidelobes. Other decoding algorithms such as back projection should improve performance, as would using complementary masks, but these have not been implemented. There may be conditions in which the diffraction patterns becomes invertible, in which case the SPSF would have zero sidelobes, a most desirable condition, but these have yet to be identified. Further investigation into exploiting the diffraction pattern's symmetrical properties may lead to a solution and should be a topic of future investigation.

This study was done for 800 nm monochromatic radiation. Opening up the bandpass to $\Delta\lambda$=100 nm will promote more throughput but will also degrade resolution due to dispersion. The effect of dispersion, although theoretically understood, needs to be verified by future analysis and experiment.

Before coded apertures can successfully be applied to NVGs, a better understanding is needed of its diffraction pattern characteristics and the relationship to the SPSF. It may also be possible to modify the aperture function in such a way as to yield a more ideal system response.

REFERENCES

[1] Fenimore, E. E., and Cannon, T. M., "Coded aperture imaging with Uniformly Redundant Arrays," Appl. Opt. 17, 337 (1978).
[2] Lewis, Keith, "Adaptive masks for discriminative coded aperture imaging," Proc. of SPIE Vol. 7818, 781803, (2010)
[3] Gordon, Neil T., de Villiers, Geoffrey D., Ridley, Kevin D., Bennett, Charlotte R., McNie, Mark E., Proudler, Ian K., Russell, Lee, Slinger, Christopher W., and Gilholm, Kevin, "An experimental infrared sensor using adaptive coded apertures for enhanced resolution," Proc. of SPIE Vol. 7818, 781806, (2010).
[4] Gottesman, Stephen R., and Fenimore, E. E., "New family of binary arrays for coded aperture imaging," Appl. Opt., 28, 4344 (1989).
[5] Gottesman, Stephen R., "Coded apertures: past, present, and future applications and design," Proc. of SPIE 6714-05 (2007).
[6] Gottesman, Stephen R., Isser, Abraham, Gigioli Jr., George W., "Adaptive coded apertures: bridging the gap between non-diffractive and diffractive imaging systems," Proc. of SPIE Vol. 7818, 781805 (2010)
[7] Martin, Liz, and Clark, Jeff, "Physics Based Simulation of Night Vision Goggles," IMAGE 2000 Conference, Scottsdale, Arizona 10-14 July 2000.
[8] Zemax-EE (64 bit) Version April 14, 2010, http://zemax.com/